Development of Non-Reflective Boundary Handling for the Quasi-One-Dimenional Flow Model in the Radical Novelties Engine Simulation

Richard C. Wagner
Aerospace Engineer

Introduction:

During the development of my piston engine design and analysis simulation, a surprising issue arose when I was performing mesh-independence studies. The simulation models the flows through intake and exhaust pipes as quasi-one-dimensional flows. As such, each pipe is decomposed into multiple cells that run axially, down the length of the pipe. Typically, in any such CFD model, as the number of cells is increased, the results will converge onto a final solution. When that solution is reached, the simulation is said to have reached a point of grid- or mesh-independence, and usually, adding more cells won't improve the fidelity of the solution. In the case of the engine simulation, I found just the opposite occurring. As I added cells, the simulation's fidelity dropped.

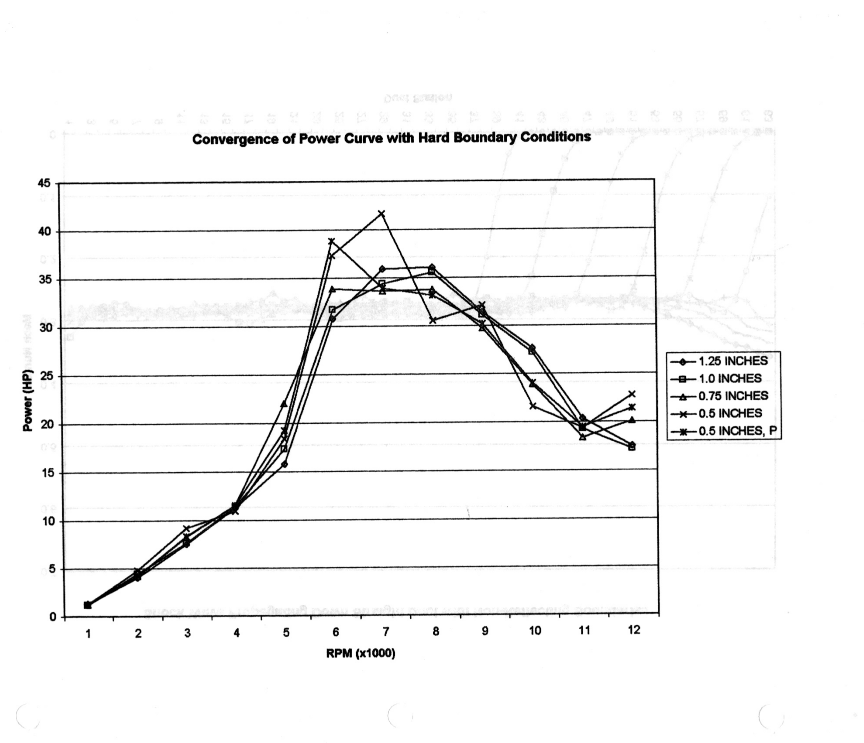

Figure 1: The Effect of Finer Mesh Size on the Power Curve

Figure 1 shows a series of power curves for a single-cylinder engine, measured from 1,000 through 12,000 rpm. For each successive curve, more cells are added to the intake and exhaust pipes, making the length of the cells in the pipe meshes smaller. As each mesh is made finer, from a cell length of 1.25 inches to a cell length of 0.5 inches, the results actually get *worse*, exhibiting peaks and notches. This is just the opposite of what I expected.

After a great deal of analysis, I determined that this behavior was being caused by the boundary handling at the atmospheric end of the pipes. The early handling at the atmospheric end was simple, maintaining constant, atmospheric pressure at that end. That kind of handling works well as long as the flow is subsonic or steady, supersonic. However, when the flow is unsteady and ranging from subsonic through supersonic--and especially including shock and expansion waves--it is insufficient.

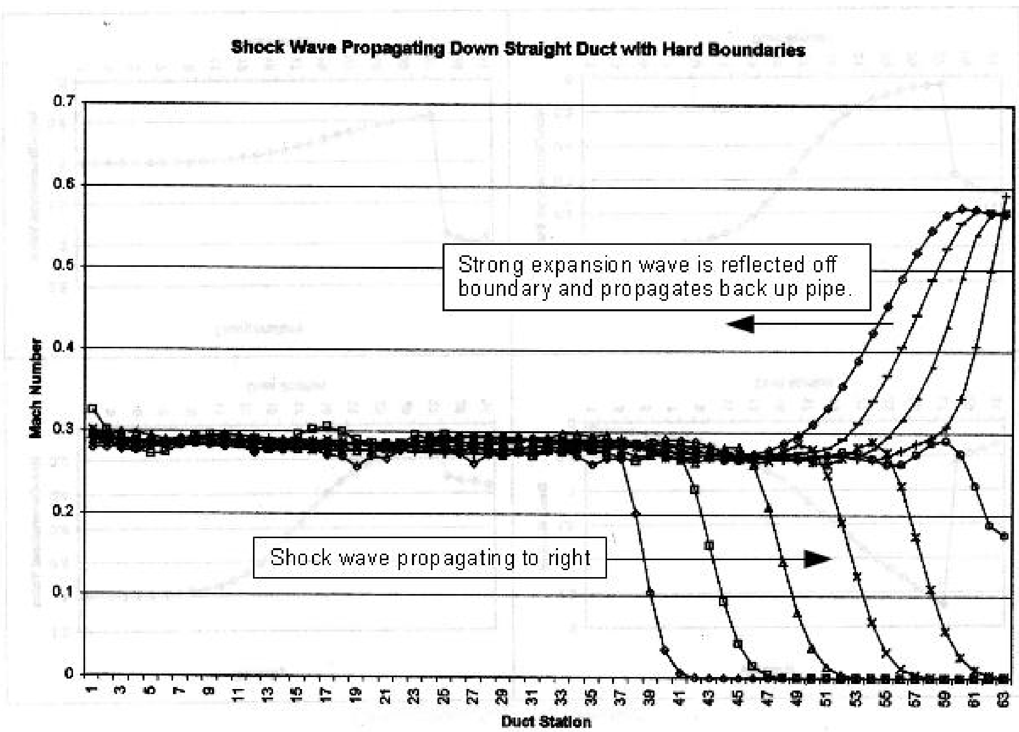

Figure 2: Shock Wave Refecting off of Constant-Pressure Boundary

In Figure 2, a shock wave is propagating from left to right down an exhaust pipe. The atmospheric end is on the right of the figure, and we pick up the wave already in transit. When the shock wave reaches the "hard", constant-pressure boundary, it is reflected back up the pipe as a strong expansion wave. This doesn't happen in reality. When this scenario occurs in a real pipe, the shock wave exits the pipe, then passes out, into the atmosphere, expanding in three dimensions. A strong expansion wave *isn't* reflected back up the pipe.

Under most operating conditions, when the exhaust valve of a piston engine begins to open, the pressure inside of the cylinder is much higher than atmospheric pressure, stimulating the production of a shock wave at the valve, which can then pass through the pipe. And so shock waves are generated in most engine exhaust systems with regularity. The simulation models the first part of this process, the propagation of the shock wave, correctly. But when the wave reaches the end of the pipe, the simulation is predicting a non-physical phenomenon, the reflection of the strong expansion wave. In the simulation, the presence of the expansion wave and its passage back up the pipe produces erroneous dynamics in the flow, affecting the power curve results. With a coarse computational mesh, the shock wave is softened as it passes down the pipe by the numerical dissipation of the time-marching solution. By the time the wave reaches the end of the pipe, it is significantly weakened and hence, so is the reflected expansion wave. But as the mesh is made finer, the shock is resolved with greater accuracy and dissipates less, making the reflected expansion stronger. After considering this situation, I realized that I needed to implement some form of "non-reflective" boundary handling to make the simulation of the pipe flows more realistic.

The following pages, taken directly from my development notes, detail the derivation and development of non-reflective boundary handling for the engine simulation. This is just one small facet of the work that makes up the engine simulation, and it took about three months of full-time work to research, understand, derive and apply what you see here. My research began with the seminal work of Thompson[1]; and then continued with more contemporary papers by Sumi, Kurotaki and Hiyami[2]; Selle, Nicoud and Poinsot[3]; Anderson, Thomas and Van Leer[4], Bogey and Bailly[5]; and Rohde[6]. I also had a number of email discussions with Dr. Nicoud, which were quite illuminating.

In the end, I developed a system of characteristically-based equations that could be used to calculate the rates of change of the primitive flow variables--pressure, density and velocity--and could then be used to calculate the rates of change of the conservative, flux variables at the pipe exits. The new handling is only applied to the endmost cell of each pipe, and only to calculate the flux variable rates. Integration of those values to the flux variables is carried out along with that for the field cells. The calculation of the flux variable rates for the field cells is handled as it was before this work was accomplished.

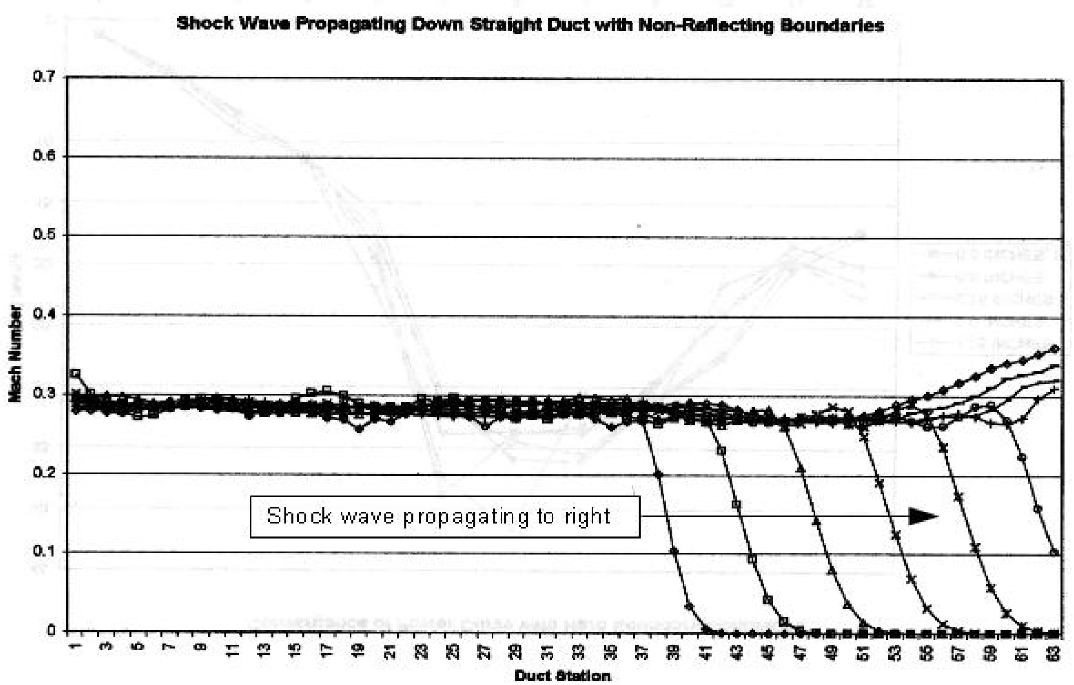

Figure 3: Shock Wave Passing out of Exhaust Pipe

The results were pleasing. In Figure 3, you can see the same scenario that was run in Figure 2, but with the new boundary handling in place. Note how much weaker the reflected expansion wave is. The new, non-reflective boundary handling allows the shock wave to exit the pipe.

Finally, figure 4 shows the effect of the new handling on the power curves of the same single-cylinder engine from Figure 1. Now, as the numerical mesh is made finer, we see the curves converging onto a single solution. This is just the result I was hoping for.

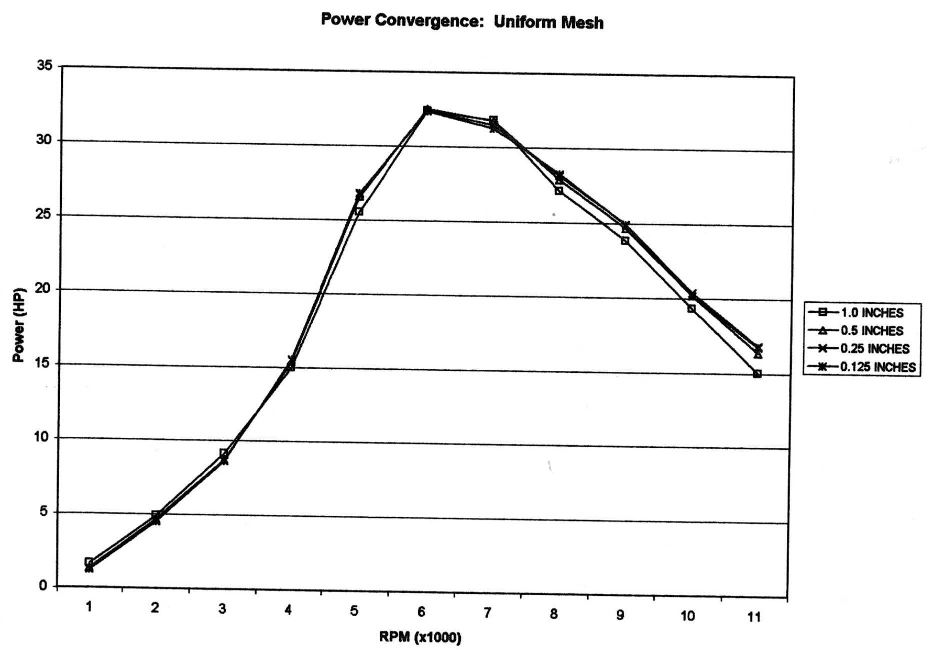

Figure 4: Power Curves with Non-Reflective Boundary Handling in Place

The results page from my notes is on page 17, where you'll find a bit more discussion. I hope the scans of my notes are legible. Please feel free to call or write with any questions.

Regards,

Rich

References

1. K. Thompson, “Time Dependent Boundary Conditions for Hyperbolic Systems”, Journal of Computational Physics, Vol. 68, 1987, pp. 1-24.
2. T. Sumi, et al, "Generalized Characteristic Interface Conditions for Accurate Multi-block Computation" 44th AIAA Aerospace Sciences Meeting, AIAA 2006-1272
3. L. Selle, et al, "Actual Impedence of Nonreflecting Boundary Conditions: Implications for Computation of Resonators", AIAA Journal, Vol 42, No. 5, May 2004, pp. 958-964.
4. W. Anderson, et al, "Comparison of Finite Volume Flux Vector Splittings for the Euler Equations", AIAA Journal, Vol. 24, No. 9, Sept. 1986, pp. 1453-1460.
5. C. Bogey and C. Bailly, "Three-dimensional non-reflective boundary conditions for acoustic simulations: far field formulation and validation test cases", Acta Acoustica United with Acoustica, Vol. 88, 2002, pp. 463-471.
6. A. Rohde, "Eigenvalues and Eigenvectors of the Euler Equations in General Geometries", AIAA, 2001-2609.

Quasi-One-Dimensional, Non-Reflective Boundary Handling:

To implement non-reflective boundaries, we again perform a characteristic analysis on the governing equations. For this case, let's use the equations for quasi-one-dimensional flow:

$$\frac{\partial}{\partial t}(\rho A) + \frac{\partial}{\partial x}(\rho A V) = 0$$

$$\frac{\partial}{\partial t}(\rho A V) + \frac{\partial}{\partial x}(\rho V^2 A) = -A\frac{\partial P}{\partial x}$$

$$\frac{\partial}{\partial t}\left[\rho\left(c_v T + \frac{V^2}{2}\right)A\right] + \frac{\partial}{\partial x}\left[\rho V A\left(c_v T + \frac{V^2}{2}\right)\right] = -\frac{\partial}{\partial x}(PAV)$$

These equations are in conservation form. I have found that the equations must be converted to non-conservation form, with dependent variables ρ, u, and P, to perform the analysis. In this new form, we have:

$$\frac{\partial \rho}{\partial t} + u\frac{\partial \rho}{\partial x} + \rho\frac{\partial u}{\partial x} + \frac{\rho u}{A}\frac{\partial A}{\partial x} = 0 \qquad \text{(\underline{Verified correct})}$$

$$\frac{\partial u}{\partial t} + u\frac{\partial u}{\partial x} + \frac{1}{\rho}\frac{\partial P}{\partial x} = 0$$

$$\frac{\partial P}{\partial t} + \rho c^2\frac{\partial u}{\partial x} + u\frac{\partial P}{\partial x} + \frac{\rho c^2 u}{A}\frac{\partial A}{\partial x} = 0$$

Even in this form, we can write a generic equation which represents this system:

$$\frac{\partial U}{\partial t} + a\frac{\partial U}{\partial x} + J = 0$$

Note the form of this equation. It is <u>already</u> in the form of a wave equation. The matrix a is easy to derive, just by inspection:

$$a = \begin{bmatrix} u & \rho & 0 \\ 0 & u & \frac{1}{\rho} \\ 0 & \rho c^2 & u \end{bmatrix}$$

(The equations were converted to non-conservation form using the accompanying Maxima program.)

The eigenvalues for this matrix are:

$$\lambda_1 = u - c \qquad \lambda_2 = u + c \qquad \lambda_3 = u$$

And the eigenvalue matrix is:

$$\Lambda = \begin{bmatrix} u-c & 0 & 0 \\ 0 & u+c & 0 \\ 0 & 0 & u \end{bmatrix}$$

$$R = \begin{bmatrix} 1 & 1 & 1 \\ -\frac{c}{\rho} & \frac{c}{\rho} & 0 \\ c^2 & c^2 & 0 \end{bmatrix}$$

The left eigenvector matrix is:

$$L = R^{-1} = \begin{bmatrix} 0 & -\frac{\rho}{2c} & \frac{1}{2c^2} \\ 0 & \frac{\rho}{2c} & \frac{1}{2c^2} \\ 1 & 0 & -\frac{1}{c^2} \end{bmatrix}$$

We'll transform the original, generic wave equation into a characteristic wave equation by applying the Black Magic Left Eigenvector Trick (see CFD notes).

$$[L]\frac{\partial U}{\partial t} + [\Lambda][L]\frac{\partial U}{\partial x} + [L]\{J\} = 0$$

$$\frac{\partial U}{\partial t} = \begin{Bmatrix} \frac{\partial \rho}{\partial t} \\ \frac{\partial u}{\partial t} \\ \frac{\partial P}{\partial t} \end{Bmatrix}$$

$$[L]\frac{\partial U}{\partial t} = \begin{Bmatrix} -\frac{\rho}{2c}\frac{\partial u}{\partial t} + \frac{1}{2c^2}\frac{\partial P}{\partial t} \\ \frac{\rho}{2c}\frac{\partial u}{\partial t} + \frac{1}{2c^2}\frac{\partial P}{\partial t} \\ \frac{\partial \rho}{\partial t} - \frac{1}{c^2}\frac{\partial P}{\partial t} \end{Bmatrix}$$

$$\frac{\partial U}{\partial x} = \begin{Bmatrix} \dfrac{\partial \rho}{\partial x} \\[2ex] \dfrac{\partial u}{\partial x} \\[2ex] \dfrac{\partial P}{\partial x} \end{Bmatrix} \qquad [L]\,\frac{\partial U}{\partial x} = \begin{Bmatrix} -\dfrac{\rho}{2c}\dfrac{\partial u}{\partial x} + \dfrac{1}{2c^2}\dfrac{\partial P}{\partial x} \\[2ex] \dfrac{\rho}{2c}\dfrac{\partial u}{\partial x} + \dfrac{1}{2c^2}\dfrac{\partial P}{\partial x} \\[2ex] \dfrac{\partial \rho}{\partial x} - \dfrac{1}{c^2}\dfrac{\partial P}{\partial x} \end{Bmatrix}$$

$$J = \begin{Bmatrix} \dfrac{\rho u}{A}\dfrac{\partial A}{\partial x} \\[2ex] 0 \\[2ex] \dfrac{\rho c^2 u}{A}\dfrac{\partial A}{\partial x} \end{Bmatrix} \qquad [L]\{J\} = \begin{Bmatrix} \dfrac{1}{2\cancel{c^2}}\dfrac{\rho \cancel{c^2} u}{A}\dfrac{\partial A}{\partial x} \\[2ex] \dfrac{1}{2\cancel{c^2}}\dfrac{\rho \cancel{c^2} u}{A}\dfrac{\partial A}{\partial x} \\[2ex] \dfrac{\rho u}{A}\dfrac{\partial A}{\partial x} - \dfrac{1}{\cancel{c^2}}\dfrac{\rho \cancel{c^2} u}{A}\dfrac{\partial A}{\partial x} \end{Bmatrix}$$

And the new characteristic wave equations are:

$$-\frac{\rho}{2c}\frac{\partial u}{\partial t} + \frac{1}{2c^2}\frac{\partial P}{\partial t} + (u-c)\left(-\frac{\rho}{2c}\frac{\partial u}{\partial x} + \frac{1}{2c^2}\frac{\partial P}{\partial x}\right) + \frac{\rho u}{2A}\frac{\partial A}{\partial x} = 0$$

$$\frac{\rho}{2c}\frac{\partial u}{\partial t} + \frac{1}{2c^2}\frac{\partial P}{\partial x} + (u+c)\left(\frac{\rho}{2c}\frac{\partial u}{\partial x} + \frac{1}{2c^2}\frac{\partial P}{\partial x}\right) + \frac{\rho u}{2A}\frac{\partial A}{\partial x} = 0$$

$$\frac{\partial \rho}{\partial t} - \frac{1}{c^2}\frac{\partial P}{\partial t} + u\left(\frac{\partial \rho}{\partial x} - \frac{1}{c^2}\frac{\partial P}{\partial x}\right) = 0$$

We can clean these up a bit by multiplying on both sides:

$$-\rho c \frac{\partial u}{\partial t} + \frac{\partial P}{\partial t} + (u-c)\left(-\rho c \frac{\partial u}{\partial x} + \frac{\partial P}{\partial x}\right) + \frac{\rho u c^2}{A}\frac{\partial A}{\partial x} = 0$$

$$\rho c \frac{\partial u}{\partial t} + \frac{\partial P}{\partial t} + (u+c)\left(\rho c \frac{\partial u}{\partial x} + \frac{\partial P}{\partial x}\right) + \frac{\rho u c^2}{A}\frac{\partial A}{\partial x} = 0$$

$$c^2 \frac{\partial \rho}{\partial t} - \frac{\partial P}{\partial t} + u\left(c^2 \frac{\partial \rho}{\partial x} - \frac{\partial P}{\partial x}\right) = 0$$

or, naming the spatial terms:

$$\boxed{\begin{aligned} \mathcal{L}_1 &= (u-c)\left(-\rho c \frac{\partial u}{\partial x} + \frac{\partial P}{\partial x}\right) \\ \mathcal{L}_2 &= (u+c)\left(\rho c \frac{\partial u}{\partial x} + \frac{\partial P}{\partial x}\right) \\ \mathcal{L}_3 &= u\left(c^2 \frac{\partial \rho}{\partial x} - \frac{\partial P}{\partial x}\right) \end{aligned}}$$

Then the characteristic equations are:

$$-\rho c \frac{\partial u}{\partial t} + \frac{\partial P}{\partial t} + \frac{\rho u c^2}{A}\frac{\partial A}{\partial x} + \mathcal{L}_1 = 0 \qquad (1)$$

$$\rho c \frac{\partial u}{\partial t} + \frac{\partial P}{\partial t} + \frac{\rho u c^2}{A}\frac{\partial A}{\partial x} + \mathcal{L}_2 = 0 \qquad (2)$$

$$c^2 \frac{\partial \rho}{\partial t} - \frac{\partial P}{\partial t} + \mathcal{L}_3 = 0 \qquad (3)$$

Adding (1) and (2), we have:

$$2\frac{\partial P}{\partial t} + 2\frac{\rho u c^2}{A}\frac{\partial A}{\partial x} + \mathcal{L}_1 + \mathcal{L}_2 = 0$$

or,

$$\boxed{\frac{\partial P}{\partial t} + \frac{\rho u c^2}{A}\frac{\partial A}{\partial x} + \frac{1}{2}\left(\mathcal{L}_1 + \mathcal{L}_2\right) = 0}$$

Rearranging this, we have:

$$\frac{\partial P}{\partial t} = -\frac{\rho u c^2}{A}\frac{\partial A}{\partial x} - \frac{1}{2}\left(\mathcal{L}_1 + \mathcal{L}_2\right) = 0$$

Substituting this into (3),

$$c^2\frac{\partial \rho}{\partial t} + \frac{\rho u c^2}{A}\frac{\partial A}{\partial x} + \frac{1}{2}\left(\mathcal{L}_1 + \mathcal{L}_2\right) + \mathcal{L}_3 = 0$$

or,

$$\boxed{\frac{\partial \rho}{\partial t} + \frac{\rho u}{A}\frac{\partial A}{\partial x} + \frac{1}{c^2}\left[\frac{1}{2}\left(\mathcal{L}_1 + \mathcal{L}_2\right) + \mathcal{L}_3\right]}$$

Last, subtracting (2) - (1),

$$2\rho c\frac{\partial u}{\partial t} + \mathcal{L}_2 - \mathcal{L}_1 = 0$$

or,

$$\boxed{\frac{\partial u}{\partial t} + \frac{1}{2\rho c}\left(\mathcal{L}_2 - \mathcal{L}_1\right) = 0}$$

Our equations are in conservation form, however, and so, we can convert these three equations by:

$$\frac{\partial U_1}{\partial t} = \frac{\partial}{\partial t}(\rho \bar{A}) = \bar{A}\,\frac{\partial \rho}{\partial t}$$

$$\boxed{\frac{\partial U_1}{\partial t} = \bar{A}\,\frac{\partial \rho}{\partial t}}$$

$$\frac{\partial U_2}{\partial t} = \frac{\partial}{\partial t}(\rho V \bar{A}) = \bar{A}\,\frac{\partial}{\partial t}(\rho V) = \bar{A}\left(V\frac{\partial \rho}{\partial t} + \rho\frac{\partial V}{\partial t}\right)$$

$$\boxed{\frac{\partial U_2}{\partial t} = \bar{A}\left(V\frac{\partial \rho}{\partial t} + \rho\frac{\partial V}{\partial t}\right)}$$

$$\frac{\partial U_3}{\partial t} = \frac{\partial}{\partial t}(\rho E \bar{A}) = \bar{A}\,\frac{\partial}{\partial t}(\rho E) = \bar{A}\left(E\frac{\partial \rho}{\partial t} + \rho\frac{\partial E}{\partial t}\right)$$

$$E = c_v T + \frac{V^2}{2} \qquad P = \rho R T \Rightarrow T = \frac{P}{\rho R} \Rightarrow E = \frac{c_v}{R}\frac{P}{\rho} + \frac{V^2}{2}$$

$$\frac{\partial E}{\partial t} = \frac{c_v}{R}\frac{\partial}{\partial t}\left(\frac{P}{\rho}\right) + \frac{1}{2}\frac{\partial}{\partial t}(V^2) = \frac{c_v}{R}\left(\frac{1}{\rho}\frac{\partial P}{\partial t} - \frac{P}{\rho^2}\frac{\partial \rho}{\partial t}\right) + V\frac{\partial V}{\partial t}$$

$$\boxed{\frac{\partial U_3}{\partial t} = \bar{A}\left[\left(\frac{c_v}{R}\frac{P}{\rho} + \frac{V^2}{2}\right)\frac{\partial \rho}{\partial t} + \frac{c_v}{R}\left(\frac{\partial P}{\partial t} - \frac{P}{\rho}\frac{\partial \rho}{\partial t}\right) + \rho V\frac{\partial V}{\partial t}\right]}$$

We'll use these equations, along with the three equations for the primative rates, to calculate the rates at the boundaries.

For the N^{th} end, for a subsonic outflow, the characteristics look like:

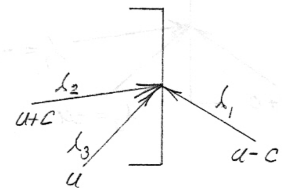

λ_2 and λ_3 carry influences from within the domain, and so $\mathcal{L}_2$ and $\mathcal{L}_3$ can be calculated using one-sided, rearward differences. λ_1 carries influences into the domain from the outside. We can't calculate $\mathcal{L}_1$, so we'll instead calculate it by:

$$\mathcal{L}_1 = K\,(p - p_\infty)$$

$$K = \pi\,(1 - M_N^2)\, c_N / L$$

This will give us the non-reflective condition.

For a supersonic outflow, the characteristics are:

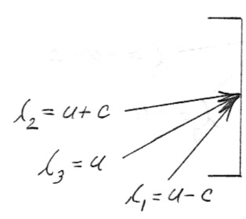

λ_1 is now positive, and so $\mathcal{L}_1$ is now calculated as $\mathcal{L}_2$ and $\mathcal{L}_3$, using one-sided, rearward differences.

For a subsonic inflow, the characteristics are:

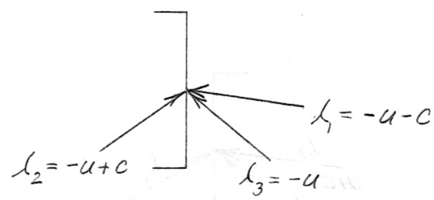

λ_2 is positive, so we'll calculate $\mathcal{L}_2$ from the interior. We'll again calculate $\mathcal{L}_1$ from the pressure differential, and $\mathcal{L}_3$ by:

$$\mathcal{L}_3 = K(\rho - \rho_\infty)$$

$$K = \pi (1 - M_N^2)\, c_N / L$$

By always calculating λ_2 from the interior, the inlet velocity will be 'automatically limited to' $M \leq 1$.

For the 0th end, for a subsonic outflow,

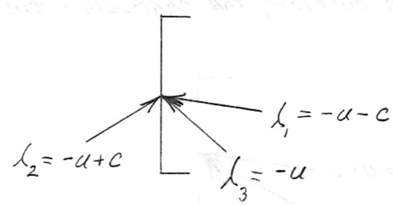

λ_1 and λ_3 are negative. $\mathcal{L}_1$ and $\mathcal{L}_3$ carry influences from within the domain, and so we'll calculate them from the interior. λ_2 is positive. $\mathcal{L}_2$ carries influences from outside. We'll calculate it using the pressure differential.

For a supersonic outflow, we'll calculate $\mathcal{L}_2$ from the interior.

For a subsonic inflow,

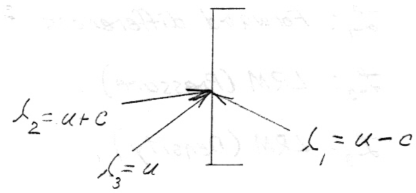

λ_1 is negative. $\mathcal{L}_1$ carries influences from within the domain, and so we'll calculate it from the interior. By always calculating it from the interior, the inflow velocity will be limited to $M=1$. λ_2 and λ_3 are positive. $\mathcal{L}_2$ and $\mathcal{L}_3$ carry influences from outside. We'll calculate $\mathcal{L}_2$ using the pressure differential and $\mathcal{L}_3$ using the density differential.

Nth End:

$u \geq 0$:

$\mathcal{L}_1$:

$u<c$: Linear Relation Method (Pressure)

$u \geq c$: Rearward differences

$\mathcal{L}_2$: Rearward differences

$\mathcal{L}_3$: Rearward differences

$u<0$:

$\mathcal{L}_1$: LRM (Pressure)

$\mathcal{L}_2$: Rearward differences

$\mathcal{L}_3$: LRM (Density)

0^{th} End:

$u \geq 0$:

$\mathcal{L}_1$: Forward differences

$\mathcal{L}_2$: LRM (Pressure)

$\mathcal{L}_3$: LRM (Density)

$u < 0$:

$\mathcal{L}_1$: Forward differences

$\mathcal{L}_2$:

$u > -c$: LRM (Pressure)

$u \leq -c$: Forward differences

$\mathcal{L}_3$: Forward differences

Poinsot and Nicoud have found that, for a pipe with one end open to the atmosphere and one end closed (a quarter-wave pipe), that σ in the linear relation equation:

$$K = \sigma \left(1 - M^2\right) \frac{c}{L}$$

should be set to π.

But in the engine simulation, when a valve is open, our pipes are open at both ends, forming a half-wave pipe.

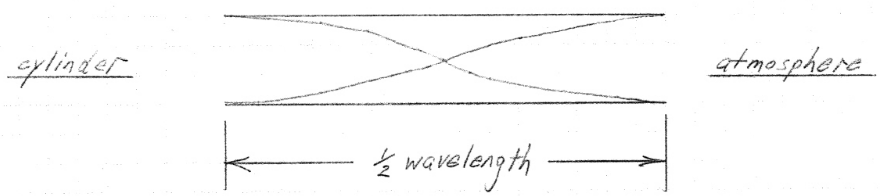

This is also true if a pipe connects to both a collector and the atmosphere.

In this case, the half-wave-mode frequency is:

$$f_0 = \left(1 - M^2\right) \frac{c}{2L}$$

And the maximum value of K that will pass this frequency is:

$$K_{max} = 4\pi \left(1 - M^2\right) \frac{c}{2L}$$

$$\boxed{K_{max} = 2\pi \left(1 - M^2\right) \frac{c}{L}}$$

And so, when we have an atmospheric pipe with a closed end, we'll use $\sigma = \pi$. With an open end, we'll use $\sigma = 2\pi$.

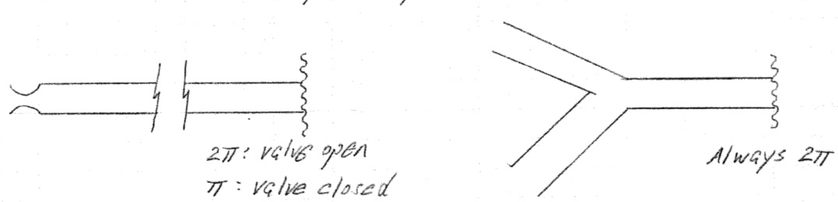

STAEDTLER® No. 937 811E Engineer's Computation Pad

To validate the non-conservation form of the equations, I've written a simulation around them.

The spatial derivatives are approximated with central difference equations. The primative states are advanced through time by the three-stage, R-K integration scheme, and artificial viscosity is applied at the end of the integration step.

The results are very good, and clearly the equations are valid. Analytically, the mach number at the shock should be 2.07 and the shock should fall between points 21 and 22. The following results are very close, and so we can be confident that our original, non-conservation-form equations, which begin our characteristic analysis, are valid. The program which embodied these equations, PRIMATIVE-DUCT.FTH, is attached.

Our final characteristic wave equations, when algebraically simplified, produce the original, non-conservation-form equations. So they are equivalent and therefore valid.

I thought that I could apply this characteristic technique to the entire domain, and not just to the endpoints. However it doesn't work. While the curves look good at first, the maximum Mach number is 2.7 instead of 2.07, and the shock falls between points 27 and 28, instead of between 21 and 22. I don't know why it doesn't work. See figure.

The results of adding this boundary handling to the tract simulation is shown on figures 3 & 4. In the third figure, a shock wave is propagating from left to right. When it reaches the right atmospheric end, it reflects and begins propagating back to the left. In the fourth figure, with non-reflective handling at the atmospheric end. In this case, the shock passes out of the duct.

The fifth figure shows the effect of the reflections on the power curve. As the mesh gets finer the results actually get worse. The sixth figure, with non-reflective handling in place, the curves converge nicely as the mesh gets finer. This is just the result we were looking for!!

Primative, Non-Conservation

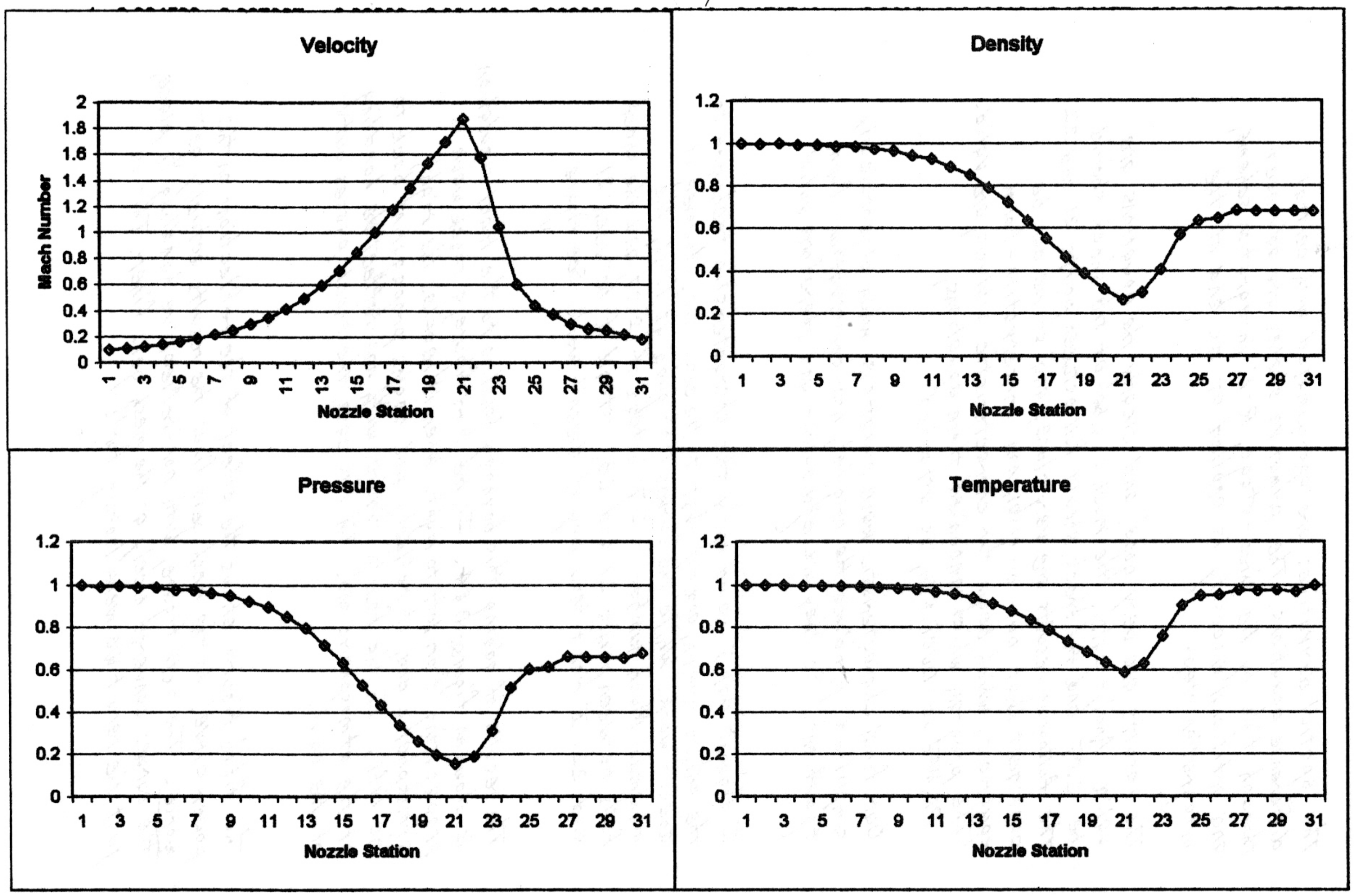

Characteristic Throughout

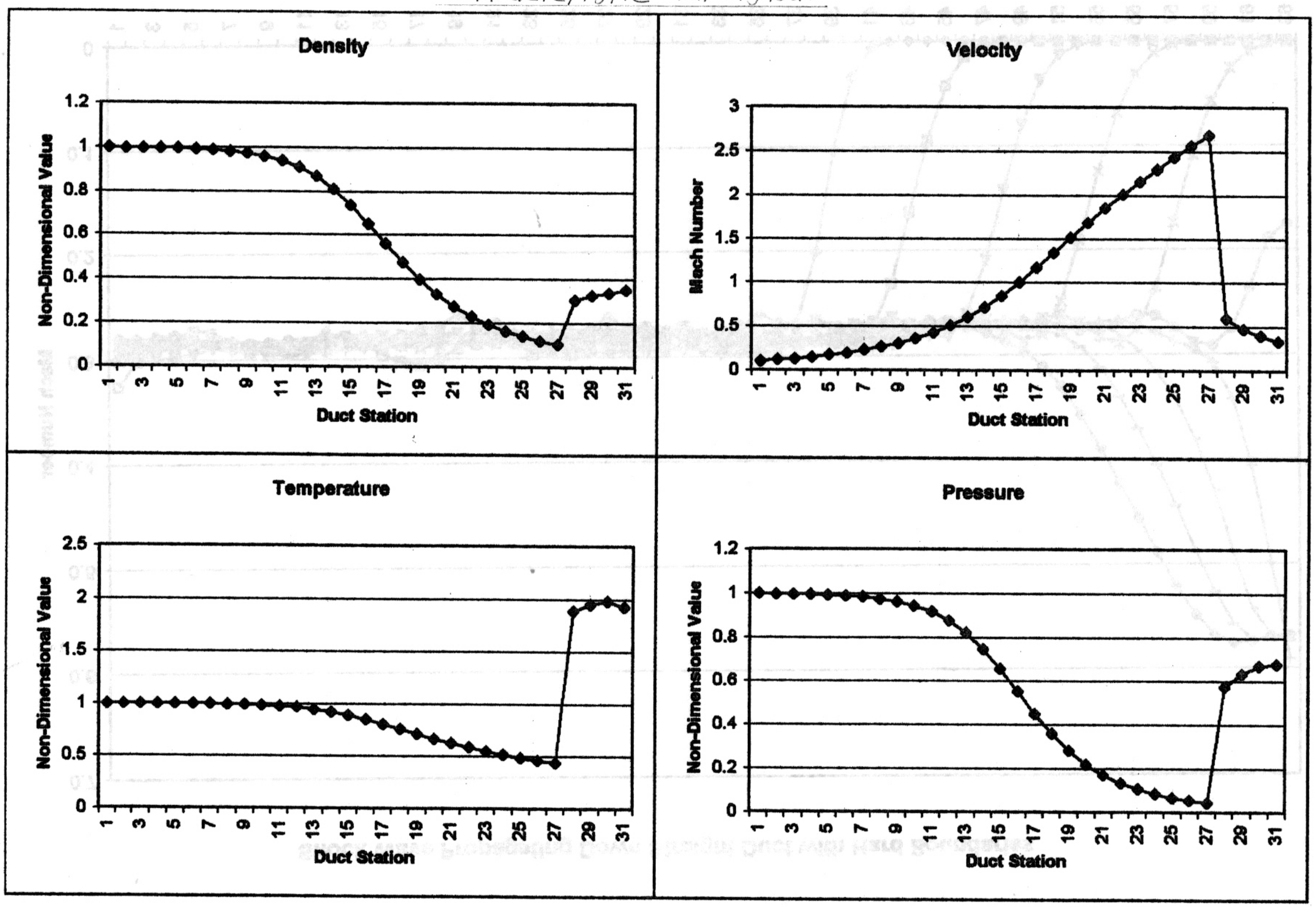

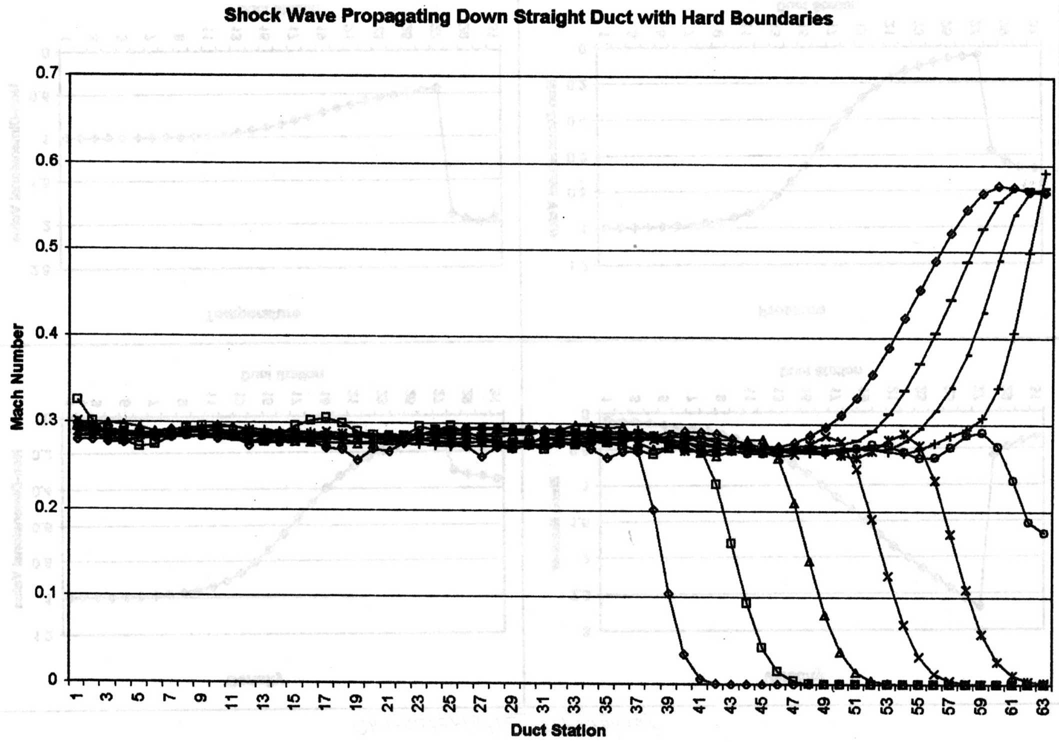
Shock Wave Propagating Down Straight Duct with Hard Boundaries
Mach Number
Duct Station
0.7
0.6
0.5
0.4
0.3
0.2
0.1
0
1
3
5
7
9
11
13
15
17
19
21
23
25
27
29
31
33
35
37
39
41
43
45
47
49
51
53
55
57
59
61
63

Shock Wave Propagating Down Straight Duct with Non-Reflecting Boundaries

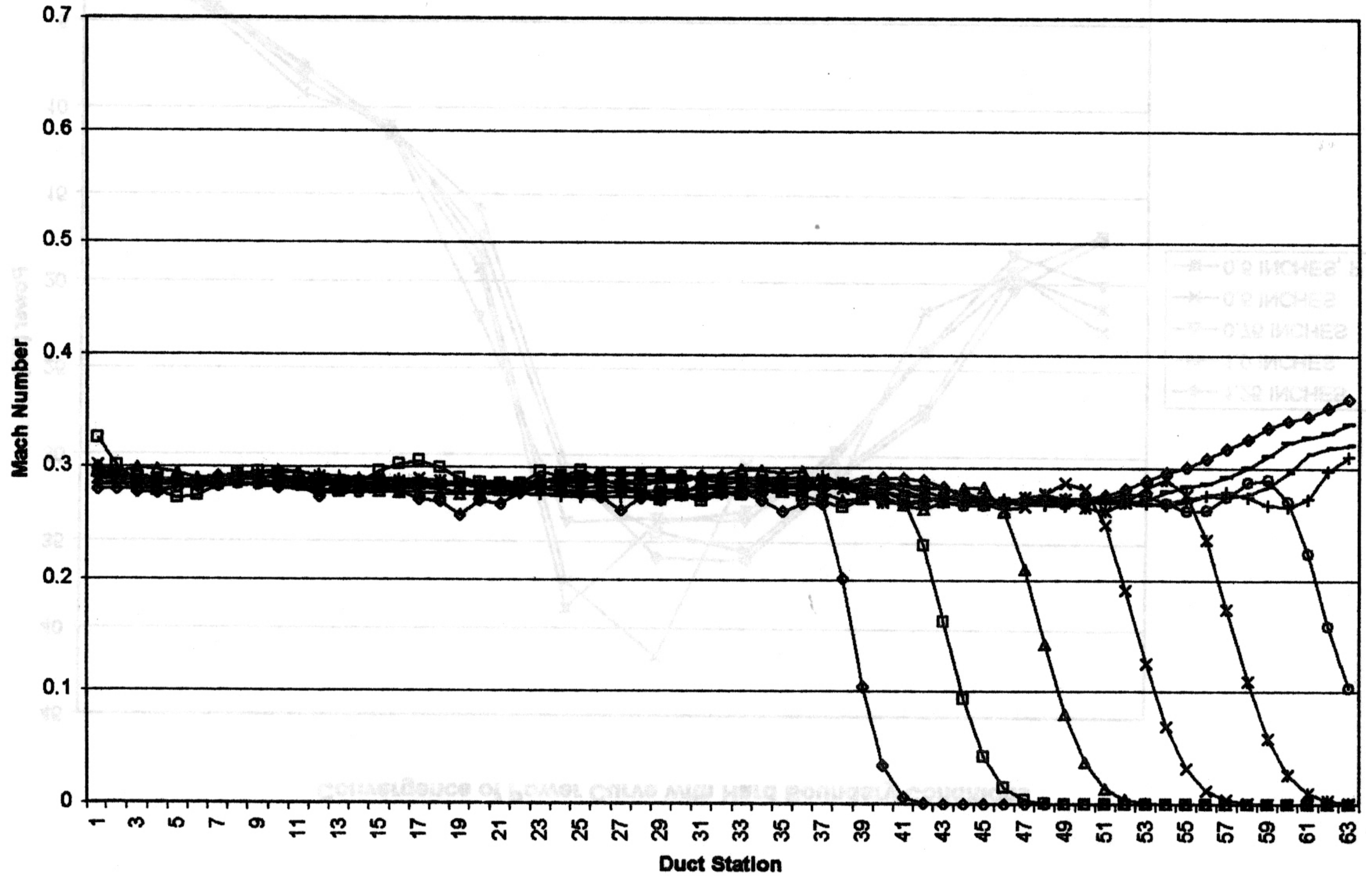

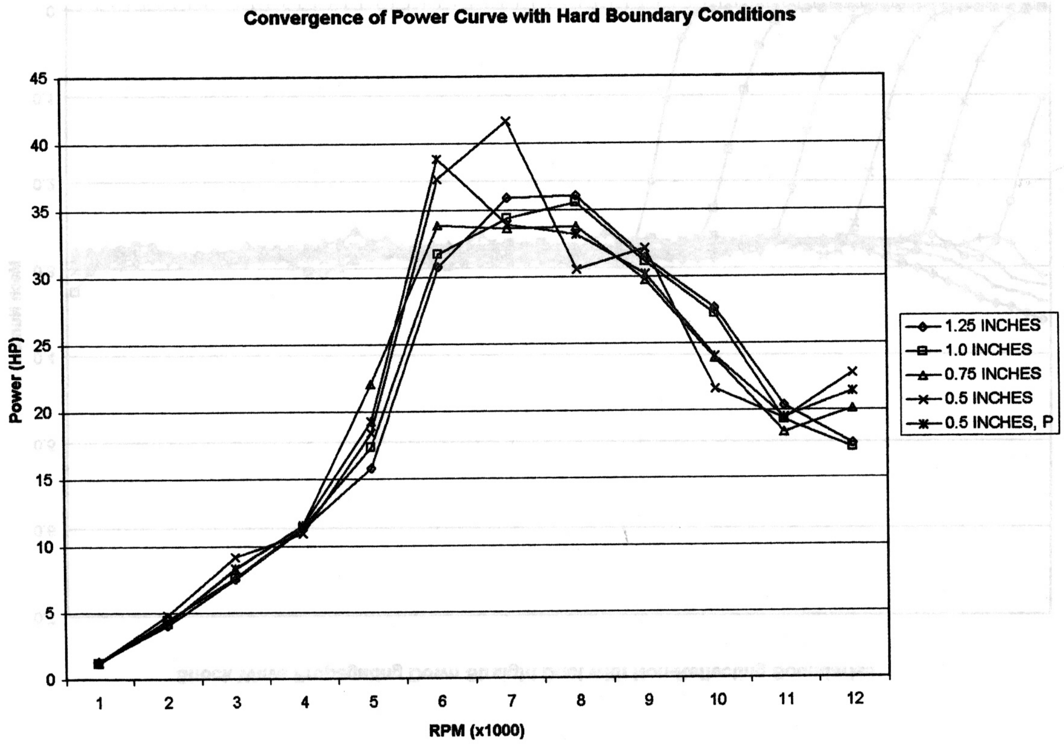
Convergence of Power Curve with Hard Boundary Conditions
Power (HP)
0
5
10
15
20
25
30
35
40
45
RPM (x1000)
1
2
3
4
5
6
7
8
9
10
11
12
1.25 INCHES
1.0 INCHES
0.75 INCHES
0.5 INCHES
0.5 INCHES, P

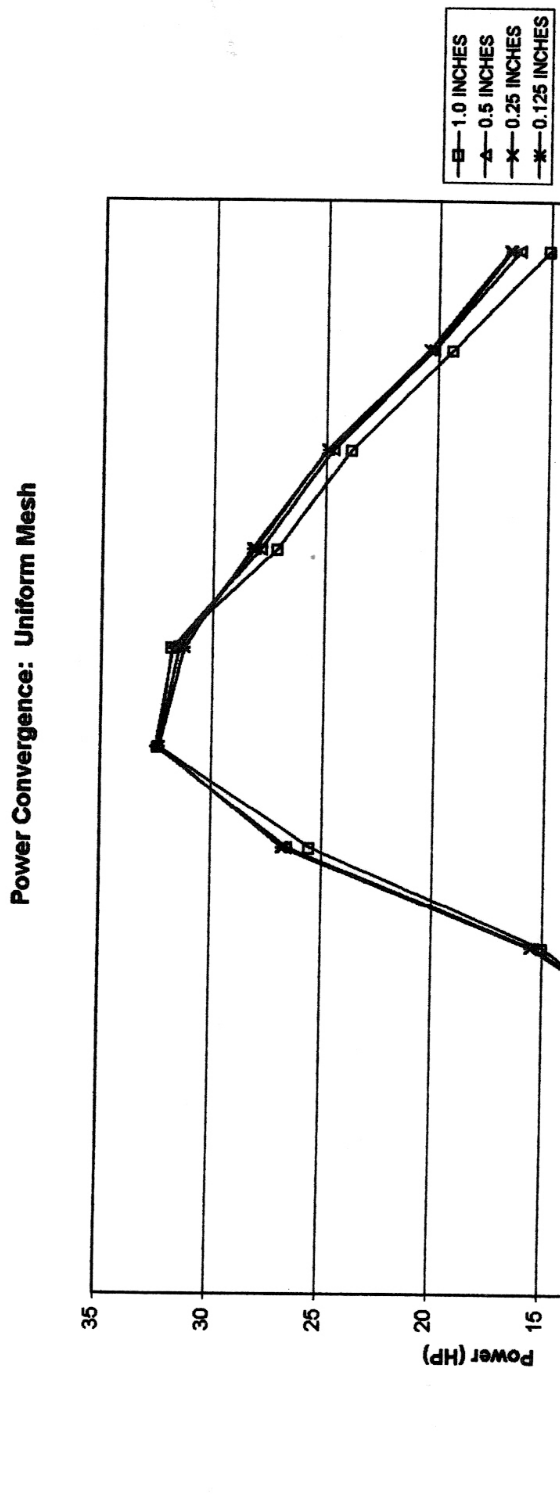
Power Convergence: Uniform Mesh
Power (HP)
RPM (x1000)
1.0 INCHES
0.5 INCHES
0.25 INCHES
0.125 INCHES
0
5
10
15
20
25
30
35
1
2
3
4
5
6
7
8
9
10
11